CARDIAC NEAR FIELD SENSORS – TECHNICAL REQUIREMENTS AND VALIDATION PROCEDURES

E. Hofer*, T. Wiener*, T. Thurner**, F. Keplinger***, P. Svasek***,
D. Sanchez-Quintana****, V. Climent****, A. Lueger*****, G. Plank*

* Medical University Graz/Institute of Biophysics, Graz, Austria
** University of Technology Graz, Institute of Electrical Measurement and Measurement Signal Processing, Graz, Austria
*** University of Technology Vienna / Institute of Industrial Electronics and Material Science, Vienna, Austria
**** University of Extremadura /Department of Human Anatomy, Badojoz, Spain
***** Medical University Graz/Department of Internal Medicine, Graz, Austria

ernst.hofer@meduni-graz.at

Abstract: Local conduction of the cardiac impulse can be described by the behaviour of the epicardial potential gradient E. With ultra-dense arrays of recording electrodes (50µm electrode spacing) and high-speed sampling with up to 800 kHz at 16-bit, E can be measured appropriately. This work describes the technical requirements on suchlike tools and the procedure of mechanical and electrical testing of this new sensor for epicardial potential gradients. High quality cardiac recording could be achieved with signal to noise ratios of 55 dB. The setup presented here can easily follow dynamic requirements of extracellular depolarisation signals. It is capable to measure potentials and cardiac near fields with outstanding precision and to resolve signal latencies of 2 µs or even less. Continuous monitoring of local conduction velocity with high resolution becomes available by means of this system.

Introduction

In cardiac electrophysiological experiments (apart from optical techniques) electrical activity is detected by means of electrodes placed at the tissue surface or with needle-like electrodes impaled in the tissue. Low resolution tools in terms of sock-like mapping systems with many electrodes (64-1000) and with inter-electrode spacing of one to several millimetres were developed in the past to explore the distribution of potentials on the heart surface [1]. Isopotential lines or isochrones representing the macroscopic excitation spread are usually computed from those datasets. At specific sites or under specific conditions the pattern of activation sequence can become very complex. This can be caused by recurrent structural discontinuities in the tissue occurring within distances less than 1 mm. Hence, substantial changes of local conduction velocity in terms of magnitude and direction than can be expected and much higher resolution for mapping systems is required.

Ultra-high density electrode arrays in the submilimeter range realized on rigid (glass) or flexible (polyamide) substrates were developed in the past and recently to get activation patterns within a limited area of observation but with high resolution [2-6]. Since the inter-electrode distances (20-100 µm) of those arrays (fig.1) are smaller than the spatial extent of the propagating depolarisation wave, bipolar recordings $\Delta\Phi = \Phi_1 - \Phi_2$, taken from two neighbouring electrodes come close to the waveform of the gradient of Φ. Therefore $\Delta\Phi$ represents the component of the electric field **E**, directed along the connecting line of the electrodes. From two pairs of electrodes arranged on orthogonal axes**,** a two dimensional representation of **E** can be computed, representing the epicardial gradient of Φ parallel to the surface. We have shown with theoretical work, that with electrode spacing (<100µm) and high sampling rates (100 kHz), direction and magnitude of local conduction velocity θ can be computed from the time course of **E**, even in case of complex conduction [7,8,9].

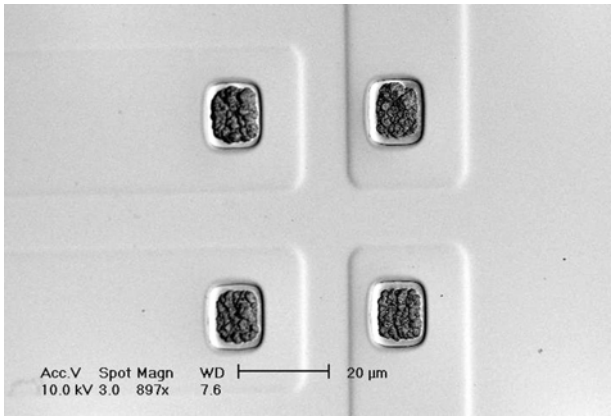

Figure 1: The electron micrograph of the near field sensor shows four recording electrodes on polyimide substrate, chlorided with Ag/AgCl.

ISSN: 1727-1983

The use of plaque electrode arrays implicates a major system problem: the unpredictable curvature (concave or convex) of the tissue surface leads either to large inter-individual variations in spacing between electrode and tissue surface or requires squeezing the array against the tissue. This restricts the space of the volume conductor proximate the surface, alters the resistance, the local currents have to pass, and induces slowing of conduction [2]. Hence widely undisturbed distribution of Φ and of **E** could only be measured with non-contact electrodes (this means no physical contact with the tissue, but indirect electrical contact via the conductive surrounding Tyrode's solution), placed near to the tissue surface, whose isolating carrier geometry would not alter the pathways of local currents substantially.

Another error inherent to mapping systems is motion artefact. The contracting heart may induce displacement between recording electrodes and tissue during contraction. Only sewed or impaled electrodes would follow the movement of the tissue. Small animal hearts (like from the mouse) with extraordinary high rates of the heartbeat (up to 600 bpm) would complicate such measurements, since the inertial forces of the moving sensor may generate additional interferences.

The endo- as well the epicardium does not represent a simple smooth surface (see fig.1), it is characterized by cavities, varying curvatures and ruffled macrostructures [10]. Thus many sites become inaccessible with conventional rigid or flexible mapping systems, since electrodes from such arrays cannot be positioned individually in 3D.

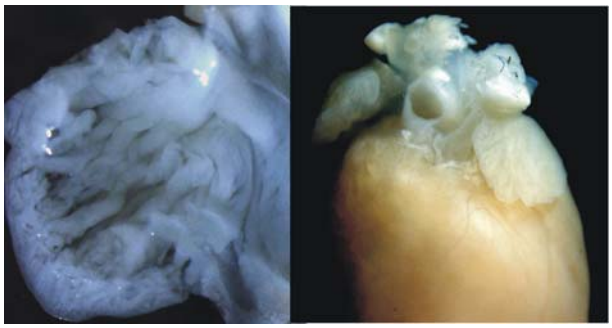

Figure 2: Complex macroscopic surface structure of the right atrial endocardium (depicted at left) and the epicardium (shown at right) of a mouse heart.

To resolve the problems mentioned above, we proposed the development of a needle-like flexible ultra-high-dense four-electrode-sensor [11]. From the signals Φ, **E** and the magnitude and the direction of θ can be computed. This work describes the testing and validation of a new flexible near-field sensor with respect to the requirements for appropriate detection of **E**.

Materials and Methods

From theoretical predictions and from experimental work with different species we expect maximum values of signal parameters, namely Φ, its derivative $d\Phi/dt$ (necessary to determine the instant of local activation LAT), potential differences $\Delta\Phi = \Phi_1 - \Phi_2$, **E** and θ respectively with 50 mV, 200 V/s, 2 mV, 200 V/m and 2 m/s.

Sensor fabrication: As substrate a polyimide film of 50 µm thickness was chosen. The electrodes, conducting lines and pads were patterned by a lift-off process with an image reversal resist. The adhesion layer of 100 nm titanium was followed by a 500 nm thick silver layer. The metal structures were isolated by a polyimide layer. Four spacer-pillars of 70 µm extent were built with epoxy-based negative photo resist around the electrodes to avoid contact of the electrodes with the tissue. Finally the electrodes were silver plated and chlorided electrochemically.

Mechanical sensor examination: We determined the mass of the sensor with a precision balance (Sartorius R300S, Germany). Bending-force-elongation curve of the carrier was measured in the range of 10 mm. Acceleration forces arising in the experiment were estimated and related to the bias forces at gentle pressure of the sensor towards the heart. The values were opposed to expected contraction forces of heart muscles, to estimate possible interference.

Data acquisition: Signals were recorded either with a 24-bit-A/D-Converter at 100 kHz. (NI PCI 4472, National Instruments, Texas) or with 800 kHz and 16-bit (DAQ PXI-6120, National Instruments, Texas). Recording was controlled by a custom designed program written in LabView 7.0 (National Instruments, Texas) and analyzed using DaDisp2000 (DSP Development Corporation, MA, USA).

Amplifier testing: First of all, the four amplifiers (x100, Bessel low pass filter 20 kHz 4th order) were tested by applying a common rectangular signal of 50 mV and 1 kHz to the all inputs (signal generator F71, Interstate Electronics Inc., New Jersey). Since small deviations of amplification would lead to misleading potential differences between the output terminals, amplification factors A were determined individually and used later for compensation. The onset of the pulse was recorded. From the four signals of Φ, we computed $d\Phi/dt$, the rise time (10-90%) of the onset $T_{10\text{-}90}$ and the instant of the steepest slope LAT (peak value of $d\Phi/dt$) for each channel.

Electrical sensor testing: The sensor was immersed in a bath, filled with conductive liquid, and connected to the amplifier system. A circular reference electrode from Ag/AgCl was mounted on the bottom of the bath. Signals were fed to a central stimulus electrode simulating local (not propagating) electrical activity in the tissue bath. This allowed us to check, if the sensor-system may follow the requirements on high-speed and high quality recording of **E**. Without stimulus signals

ISSN: 1727-1983

we determined the values of AC-interference (50 Hz), the noise level of Φ, $d\Phi/dt$, $\Delta\Phi$ and **E**.

With rectangular stimulus signals, we examined the dynamic response of the electrodes by measuring and evaluating the individual amplitudes of Φ and $d\Phi/dt$, LAT and the rise time $T_{10\text{-}90}$.

The signal was lead to the sensor in two different modes. In the first mode, the tissue bath was disconnected from the circular reference electrode and driven entirely by the potential delivered from the stimulus electrode. In the second mode, the circular reference was used as signal ground, the current pulse delivered at the stimulus electrode produced potential changes in the bath, producing a signal Φ in its vicinity. Evaluation of variation of parameters was specified generally with the median value and the range R (max-min values).

Tissue preparation: Animals (Guinea pig, mouse) were heparinised and anaesthetised with thiopental sodium (30 mg/kg), both administered intraperitoneally. Hearts were rapidly excised. Animal preparation conformed to the national ethic guidelines. The tissue was placed either in a bath filled with oxygenated Tyrode's solution (in Mm/l: NaCl 132.1, KCl 5.4, $CaCl_2$ 2.5, $MgCl_2$ 1.15, $NaHCO_3$ 24, $NaHPO_4$ 0.42, D-Glucose 5.6) flowing through at 36°C, or the whole heart was mounted on a Langendorff perfusion system.

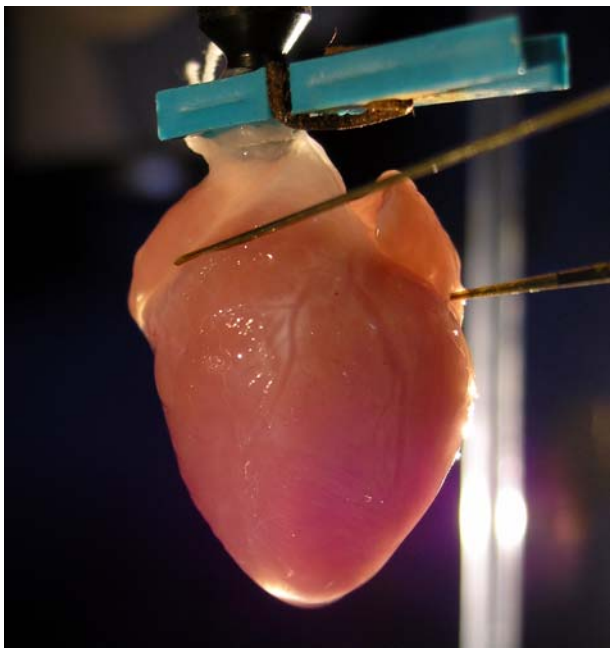

Figure 3: Isolated Guinea pig heart used as Langendorff preparation with attached cardiac near field sensor.

Biosignal recording: The heart preparation was either auto-rhythmic or paced with a point-like stimulus electrode providing a current pulse of 1 ms at an amplitude twice the rheobase. The sensor was placed with a 3D-micromanipulator at desired recording site on the tissue surface. The signals of $d\Phi/dt$, $\Delta\Phi$ and **E** were computed from Φ. Noise level of Φ was determined from a period, were no electrical activity occurred. Signal to noise ratio SNR was calculated then with

$$SNR = 20 \cdot \log(\Phi / \Phi_{noise}) \quad (1)$$

were Φ corresponds to the peak-to-peak value of the biphasic depolarisation signal and Φ_{noise} to the peak-to-peak value of noise. SNR is given in dB.

Motion artefacts: Possible displacement artefacts were detected by optical observation of the sensor and tissue movement via microscope and by checking the beat-to-beat variability of Φ, $d\Phi/dt$ and **E.**

Results

Mechanical sensor examination: The 6 cm long tongue-like sensor (weight 9.1 mg) showed linear bending force-elongation relationship (6.33 N/m, n=10, $r^2 = 0.99$). Oscillating tip movements of 5 mm amplitude (peak-to-peak) and 5 Hz would result in peak acceleration of 2.69 m/sec². Assuming that only the tip-sided third of the sensor and therefore just a tenth of the mass is involved in the full acceleration, peak inertial forces of 2.45 mN would arise. We conclude that the inertial and bias forces would not affect substantially the contraction of the heart specimen exceeding these values by far [12].

Amplifier testing: Like apparent from table 1, the inter-individual variations of Φ are very small, those of $d\Phi/dt$ are noticeable with 44.1 (44.0-44.2) mV and 2285 (2248-2310) V/s. This represents ranges of 0.42% and 2.73% of the median values. Variations of LAT and of $T_{10\text{-}90}$ larger than the sampling interval of 1.25 µs could not be found.

Table 1: Electrical parameters taken from signals applied in three different modes to the amplifier.

		CH1	*CH2*	*CH3*	*CH4*
a. Signals directly connected					
Φ	mV	44.01	44.19	44.05	44.20
$D\Phi/dt$	V/s	2248	2310	2291	2280
LAT	µs	58.75	58.75	57.50	58.75
$\Delta T_{10\text{-}90}$	µs	20.00	20.00	18.75	20.00
A		99.78	100.2	99.85	100.2
b. Signals connected via driven bath and sensor					
Φ	mV	43.05	42.92	43.13	42.93
$d\Phi/dt$	V/s	2118	2119	2143	2118
LAT	µs	160.0	160.0	158.8	158.8
$\Delta T_{10\text{-}90}$	µs	21.25	21.25	20.00	21.25
c. Signals generated by local fields					
Φ	mV	20.67	20.58	20.77	20.62
$d\Phi/dt$	V/s	861	873	880	858
LAT	µs	990.0	990.0	990.0	991.3
$\Delta T_{10\text{-}90}$	µs	30.00	28.75	28.75	30.00

ISSN: 1727-1983

Electrical sensor testing: Without stimulus signals AC-interference (peak value of the 50 Hz component of Φ) was 157 µV (148-158µV). Bipolar signals of AC-interference $\Delta\Phi$ were distinctly smaller with 8.9 µV (4.1-13.7) due to common mode rejection effects. Peak-to-peak noise of Φ, $\Delta\Phi$ and **E** was 90.2 µV (78.7-91.8) respectively 48.2 µV (41.0-55.8) and 0.96 V/m (0.82-1.12).

In the stimulus driven bath mode we obtained variations of Φ and $d\Phi/dt$ respectively 42.99 mV (42.92-43.13) and 2118 V/s (2118-2143), values comparable to the amplifier testing results. LAT and $T_{10\text{-}90}$ did not vary larger than one sample interval of 1.25 µs. The field generating mode (with a different amplitude of Φ) resulted in values of 20.64 mV (20.58-20.77), 867 V/s (858-880) for Φ and $d\Phi/dt$. LAT and $T_{10\text{-}90}$ showed no detectable latencies between the individual recordings too.

Biosignal recording: Peak-to-peak amplitudes of Φ varies depending on the recording site and on the species under study from a 1 to 30 mV. Taking a representative epicardial recording and assuming 70 µm electrode spacing, we obtained 15.5 mV, 4.73 mV, 41 V/s, 67 V/m, 38 µV and 55 dB for Φ , $\Delta\Phi$, $d\Phi/dt$, **E**, Φ_{noise} and SNR. Mechanical displacement of the sensor or signal artefacts induced mechanically could not be detected in experimental use. An example of biosignal recording and monitoring is given in figure 4.

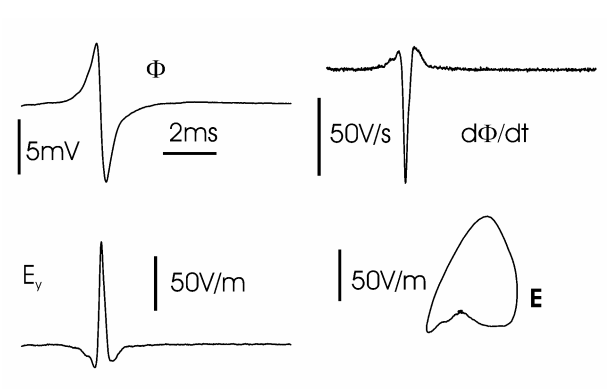

Figure 4: Signals Φ , $d\Phi/dt$, E_y and **E** recorded from the epicardium of a Guinea pig heart.

Discussion

Based on the known requirements to measure the epicardial near field **E** properly (i.e. electrode spacing <100 µm, sampling rate >100 kHz, slope detection >200V/m, SNR >40 dB like predicted [8], the microfabricated sensors were tested on their dynamic characteristic and their inter-individual matching. To obtain an accuracy of 1-2% in measuring θ, latencies in the range of 1-2 µs between the recordings have to be resolved. Despite the exact matching of all geometrical dimensions of the electrodes, there are some slight inter-individual differences in respect to noise and high-frequency response. This might be caused by variations in the electrochemical chloriding process and in small differences of lead capacitances of the sensor. However, there are no detectable phase-shifts between the channels. The rise-time (20 µs) is primarily determined by the low-pass filters of the preamplifier. The increased value of 30 µs seen in the field generated impulses is caused rather by the frequency response of the stimulus electrode than by the recording electrodes.

Conclusions

The setup presented here is capable to record potentials and cardiac near fields with outstanding precision and to resolve signal latencies with 1 µs or even less. Continuous monitoring of local conduction velocity with high resolution becomes available by means of this system [13].

Aknowledgements: The authors thank G. Gottlieb, W. Sax, G. Zach, K. Feichtinger, P. Svasek and M. Tischler for their development work and for assistance during the experiments. This work was supported by the Austrian Research Fund Grants P12293MED , R21N04, by the Austrian OEAD Grant 6/2002 and Grants SAF2004-06864 from the Spanish Ministry of Education and Science.

References

[1] ARISI G., MACCHI E., CORRADI C., LUX R.L. and TACCARDI B. (1992): 'Epicardial excitation during ventricular pacing. Relative independence of breakthrough sites from excitation sequence in canine right ventricle', *Circ. Res.*, **71**, pp. 840-849

[2] HOFER E., URBAN G., SPACH M. S., SCHAFFER-HOFER I., MOHR G. and PLATZER D. (1994): 'Measuring activation patterns of the heart at a microscopic size scale with thin-film sensors', *Am. J. Physiol.*, **266**, pp. H2136-H2145

[3] MOHR G., HOFER E. and PLANK G., (1999): 'A new real-time mapping system to detect microscopic cardiac excitation patterns', *Biomed. Instrum. Technol.*, **33**, pp. 455-461

[4] KIM C.S., UFER S., SEAGLE C.M., ENGLE C.L., TROY NAGLE H., JOHNSON T.A. and CASCIO W.E., (2004): 'Use of micromachined probes for the recording of cardiac electrograms in isolated heart tissues`, *Biosens. Bioelectron.*, **19**, pp. 1109-1116

[5] MASTROTOTARO J. J., MASSOUD H. Z., PILKINGTON T. C. and IDEKER R. E. (1992): 'Rigid and flexible thin-film multielectrode arrays for transmural cardiac recording', *IEEE Trans. Biomed. Eng.*, **39**, pp. 271-279

[6] MALKIN R.A. and PENDLEY B.D. (2000): 'Construction of a very high-density extracellular electrode array', *Am. J. Physiol. Heart Circ. Physiol.*, **279**, pp. H437-442

[7] PLANK G. and HOFER E. (2000): 'Model study of vector-loop morphology during electrical mapping of microscopic conduction in cardiac tissue', *Ann. Biomed. Eng*., **28**, pp. 1244-1252

[8] PLANK G. and HOFER E. (2003): 'Use of cardiac electric near-field measurements to determine activation times', *Ann. Biomed. Eng*., **31**, pp.1066-1076

[9] PLANK G., VIGMOND E., LEON L. J. and HOFER E. (2003): 'Cardiac near-field morphology during conduction around a microscopic obstacle - a computer simulation study`', *Ann. Biomed. Eng*., **31**, pp. 1206-1212

[10] HOFER E., PLANK G., SCHAFFERHOFER I. and SANCHEZ-QUINTANA, D., (2001): ‚Electro-anatomical characterization by cardiac electric near-fields', Proc. of 23th Annual International Conference of the IEEE Engineering in Medicine and Biology Society, Istanbul, Turkey, 2001, p.57-59

[11] HOFER E., SANCHEZ-QUINTANA D., PLANK G. and TISCHLER M., (2003): 'Normal and fractionated cardiac near-fields and their relation to micro-structure-an experimental approach', Proc. of 25th Annual International Conference of the IEEE Engineering in Medicine and Biology Society , Cancun, Mexico, 2003, p. 51-54

[12] LUNKENHEIMER P. P., REDMANN K., FLOREK J., FASSNACHT U., CRYER C. W., WUBBELING F., NIEDERER P. and ANDERSON R. H. (2004): ‚The forces generated within the musculature of the left ventricular wall', *Heart*, **90**, pp. 200-207

[13] WIENER T., THURNER T., HOFER E. and PLANK, G. (2005):'Mess-System zur Aufnahme, Visualisierung und Analyse des elektrischen Nahfeldes am Herzen', in JAMAL, R., JASCHINSKY, H.: 'Virtuelle Instrumente in der Praxis', (Hüthig GmbH&Co. KG, Heidelberg), pp.433-437

ISSN: 1727-1983